Original Article

MOLECULAR METABOLISM

Lack of resolution sensor drives age-related cardiometabolic and cardiorenal defects and impedes inflammation-resolution in heart failure

Bochra Tourki [1,4], Vasundhara Kain [1,4], Amanda B. Pullen [1], Paul C. Norris [2], Nirav Patel [1], Pankaj Arora [1], Xavier Leroy [3], Charles N. Serhan [2], Ganesh V. Halade [1,*]

ABSTRACT

Objective: Recently, we observed that the specialized proresolving mediator (SPM) entity resolvin D1 activates lipoxin A_4/formyl peptide receptor 2 (ALX/FPR2), which facilitates cardiac healing and persistent inflammation is a hallmark of impaired cardiac repair in aging. Splenic leukocyte-directed SPMs are essential for the safe clearance of inflammation and cardiac repair after injury; however, the target of SPMs remains undefined in cardiac healing and repair.

Methods: To define the mechanistic basis of ALX/FPR2 as a resolvin D1 target, ALX/FPR2-null mice were examined extensively. The systolic-diastolic heart function was assessed using echocardiography, leukocytes were phenotyped using flow cytometry, and SPMs were quantitated using mass spectrometry. The presence of cardiorenal syndrome was validated using histology and renal markers.

Results: Lack of ALX/FPR2 led to the development of spontaneous obesity and diastolic dysfunction with reduced survival with aging. After cardiac injury, ALX/FPR2$^{-/-}$ mice showed lower expression of lipoxygenases (−5, −12, −15) and a reduction in SPMs in the infarcted left ventricle and spleen, indicating nonresolving inflammation. Reduced SPM levels in the infarcted heart and spleen are suggestive of impaired cross-talk between the injured heart and splenic leukocytes, which are required for the resolution of inflammation. In contrast, cyclooxygenases (−1 and −2) were over amplified in the infarcted heart. Together, these results suggest interorgan signaling in which the spleen acts as both an SPM biosynthesizer and supplier in acute heart failure. ALX/FPR2 dysfunction magnified obesogenic cardiomyopathy and renal inflammation (↑NGAL, ↑TNF-α, ↑CCL2, ↑IL-1β) with elevated plasma creatinine levels in aging mice. At the cellular level, ALX/FPR2$^{-/-}$ mice showed impairment of macrophage phagocytic function ex-vivo with expansion of neutrophils after myocardial infarction.

Conclusions: Lack of ALX/FPR2 induced obesity, reduced the life span, amplified leukocyte dysfunction, and facilitated profound interorgan nonresolving inflammation. Our study shows the integrative and indispensable role of ALX/FPR2 in lipid metabolism, cardiac inflammation—resolution processes, obesogenic aging, and renal homeostasis.

Keywords Inflammation; Leukocytes; Myocardial infarction; Nonresolving inflammation; Obesogenic aging; Resolution of inflammation

1. INTRODUCTION

Persistent inflammation is a hallmark of coronary heart disease, especially in aging patients suffering from obesity and heart failure (HF) [1,2]. Since more than 70% of US patients are classified as overweight or obese, whether or not obesogenic aging drives nonresolving inflammation in HF remains an area of interest [1,3]. There are discrepancies in the context of the age-related obesity paradox and inflammation-resolution targets [1,4]. After cardiac injury, the identification of novel targets that regulate the inflammation and resolution cascade is critical to limit system-wide inflammation in HF [1,2]. In response to ischemia, the splenic leukocytes biosynthesize specialized proresolving mediators (SPMs) to facilitate cardiac healing; however, obesogenic aging drives nonresolving inflammation [5]. Ischemia-induced cardiac injury promotes both splenocardiac feedback signaling and cardiorenal feed-forward inflammation [6]. HF is considered a single pathology in rodent studies, but in clinical settings, it is considered an integrative and multifactorial syndrome, often superimposed on aging. Therefore, pathways targeting resolution sensors of inflammation remain an area of interest in order to delay HF post—myocardial infarction (MI) [7].

Lipoxin A_4 receptor (ALX)/formyl peptide receptor 2 (hereafter called FPR2) is a resolution sensor that plays a pivotal role in inflammation. Previous reports in experimental models highlighted the degree of

[1]Division of Cardiovascular Disease, Department of Medicine, The University of Alabama at Birmingham, Alabama, 35294, United States [2]Center for Experimental Therapeutics and Reperfusion Injury, Department of Anesthesiology, Perioperative and Pain Medicine, Brigham and Women's Hospital, Harvard Medical School Boston, Massachusetts, 02115, United States [3]Domain Therapeutics, Steinsoultz, Alsace, France

[4] Bochra Tourki and Vasundhara Kain contributed equally to this work.

*Corresponding author. Department of Medicine, Division of Cardiovascular Disease, The University of Alabama at Birmingham, 703 19th Street South, MC 7755, Birmingham, AL, 35294, United States. Fax: +1 205 975 5150. E-mail: ganeshhalade@uabmc.edu (G.V. Halade).

Received August 31, 2019 • Revision received October 14, 2019 • Accepted October 25, 2019 • Available online 16 November 2019

https://doi.org/10.1016/j.molmet.2019.10.008

Nonstandvard abbreviations

AA	arachidonic acid
ALOX-5	lipoxygenase 5
ALOX-12	lipoxygenase 12
ALOX-15	lipoxygenase 15
CRS	cardiorenal syndrome
COX-1	cyclooxygenase 1
COX-2	cyclooxygenase 2
DHA	docosahexaenoic acid
EPA	eicosapentaenoic acid
FPR2	formyl peptide receptor
GLS	global longitudinal strain
H&E	hematoxylin and eosin
HF	heart failure
KIM	kidney injury marker
LPS	lipopolysaccharide
LTB_4	leukotrienes B4
LV	left ventricle
LXA_4	lipoxin A_4
LXB_4	lipoxin B_4
MaR1	maresin 1
MaR2	maresin 2
MI	myocardial infarction
MO	months
Mrc-1	mannose receptor C-type 1
NGAL	neutrophil gelatinase-associated lipocalin
RvD1	resolvin D1
RvD4	resolvin D4
SMAα	alpha smooth muscle actin
SPMs	specialized proresolving mediators, ie, lipoxins, resolvins, maresin, and protectin families
TGFβ	transforming growth factor beta
WGA	wheat germ agglutinin

implication of FPR2 in atherosclerosis and early leukocyte recruitment after tissue injury [8–13]. However, the comprehensive role of FPR2 in cardiac repair and the inflammation–resolution processes is incomplete. Endogenous peptide annexin A1 (Ac2-26), bioactive lipids resolvin D1 (RvD1), and aspirin-triggered lipoxin (AT-LXA_4) activate FPR2 to facilitate resolution of inflammation [9,14,15]. FPR2 is highly expressed in the myeloid cell population and is activated by RvD1 at the spleen and infarcted site to expedite resolution after cardiac injury [15]. Recent studies defined the role of FPR2 in adaptive immunity as a connector between inflammation-resolution signals and B-cell biology [16,17]. FPR2 enables activated immune cells to be mobilized from the bone marrow to the injured organ, facilitating the ability to transform from physiological inflammation to resolution [10,16,18–20].

In the present study, we provide a comprehensive evaluation of the system-wide integrative role of FPR2, including its impact on survival, structure, and function of cardiometabolic and renal syndromes. Lack of FPR2 in male mice stimulated the development of early-onset, age-related obesity with reduced survival. We examined the pathological outcome in the context of (1) the cardiorenal syndrome in aging; (2) the cardiometabolic syndrome, which presents the predominant risk factors in cardiac diseases; and (3) the splenocardiac axis in acute HF to define the role of FPR2 in inflammation and resolution after MI. The current results indicate that aging drives overactivation of cyclooxygenases (COXs), leading to heart dysfunction and cardiorenal and cardiometabolic defects in aging-prone $FPR2^{-/-}$ mice. After cardiac injury, the number of resolving $Ly6C^{low}$ macrophages was decreased, amplifying unresolved inflammation with numerical expansion of neutrophils at the site of injury, because of the diminished biosynthesis of SPMs in $FPR2^{-/-}$ mice. Thus, FPR2 serves as a key resolution sensor for heart function, renal homeostasis, and lipid metabolism in cardiovascular physiology.

2. METHODS

Expanded methods and details of metabolipidomics are included in the supplementary section.

2.1. Animal care and compliance

All animal surgical procedures and treatments were conducted according to the "Guide for the Care and Use of Laboratory Animals" (8th edition, 2011) and the AVMA Guidelines for the Euthanasia of Animals (2013 edition) and were approved by the Institutional Animal Care and Use Committees at the University of Alabama at Birmingham, USA.

2.2. Human samples

Human heart tissue samples were used in compliance with the policy approved by the institutional review board at the University of Alabama at Birmingham, USA.

2.3. Generation of the ALX/$FPR2^{-/-}$ mouse

$FPR2^{-/-}$ mice were generated by homologous recombination of Cre-mediated excision in embryonic stem cells. Eight-to twelve-week old FPR2 gene locus knock-out mice homozygous on C57BL/6J background were obtained from Idorsia Pharmaceuticals Ltd, Switzerland (formerly known as Actelion Pharmaceuticals Ltd).

2.4. Flow cytometry

Single mononuclear cells were isolated from the spleen and left ventricle (LV) of wild-type (WT) and $FPR2^{-/-}$ mice and analyzed by flow cytometry as reported previously (FACs strategy Supplementary Figure 10) [21,22].

2.5. Statistical analysis

Data are expressed as mean and SEM. Statistical analyses were performed using GraphPad Prism 8. Kaplan–Meier survival test was used to analyze survival curves. One-way analysis of variance (ANOVA) or two-way ANOVA followed by Newman–Keuls post hoc test was used for multiple comparisons between d0, post-MI d1, and d5 or between 2- and 7-month controls and FPR2 groups, respectively. $p < 0.05$ was considered as statistically significant.

3. RESULTS

3.1. Human ischemic myocardium activated FPR2 expression, and mice FPR2 dysfunction induced obesity and shortened the life span

To define the integrative role of the FPR2 with regard to human ischemia pathology, we investigated three main themes (Figure 1A, study design). First, we determined the expression and location of the FPR2 protein in the human ischemic myocardium. Immunofluorescence and immunoblot analysis revealed the presence of FPR2 in the human heart (Figure 1B). In humans, FPR2 expression appears to be translocated to the cytoplasm (green and white arrows) in the ischemic

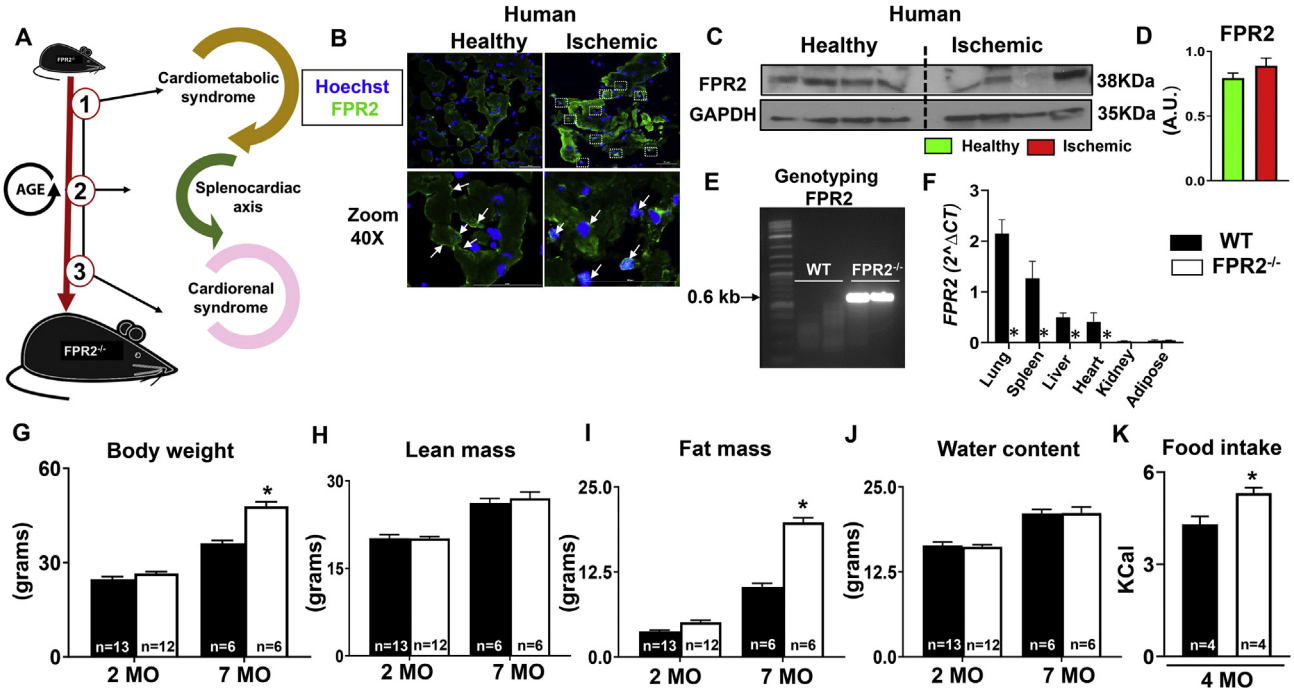

Figure 1: Human resolution sensor FPR2 translocated to cytoplasm after ischemia and deficiency of resolution sensor FPR2/ALX in mice induced obesity with enhanced mortality. **(A)** Schematic representation of the experimental design. **(B)** Immunofluorescence images showing human FPR2 translocation to the nucleus in ischemic myocardium compared with healthy myocardium. **(C, D)** Immunoblot and densitometry representing human FPR2 expression in healthy and ischemic myocardium. **(E)** PCR genotyping confirming *FPR2KO* homozygotes mice. **(F)** mRNA expression of *FPR2* in the lung, spleen, liver, LV, kidney, and fat from WT and FPR2$^{-/-}$ male mice (n = 8 mice/group; *$p < 0.05$ vs control group). Body weight and quantitative magnetic resonance imaging (QMRI) data from WT and FPR2$^{-/-}$ mice at 2 and 7 months representing **(G, H)** body weight and lean mass. **(I, J)** Fat mass and water mass. *$p < 0.001$ vs. WT. WT at 2 months, n = 13; WT at 7 months, n = 6; FPR2$^{-/-}$ at 2 months, n = 12; FPR2$^{-/-}$ at 7 months, n = 6. **(K)** Bar graph showing amplified food intake in FPR2$^{-/-}$ mice compared with WT mice (n = 4/group).

myocardium when compared with healthy human myocardium, in which FPR2 is limited to the cell membrane (green and white arrows, Figure 1B—D; human demographics provided in Supplemental Table 1 and Supplementary Figure 1). Since FPR2 is plentiful in the human ischemic heart, the precise and comprehensive role of this resolution receptor has been expanded using FPR2$^{-/-}$ mice. First, we validated the genotype of homozygote FPR2$^{-/-}$ mice using polymerase chain reaction (PCR)—based genotyping, which confirmed FPR2 deletion by the presence of the 0.6-kb band in FPR2$^{-/-}$ mice compared with WT (Figure 1E; Supplementary Figure 2A). Next, to further validate FPR2 deletion in different tissues, FPR2 mRNA expression was determined in lung, spleen, liver, heart, kidney, and adipose tissue. Real-time PCR data showed the considerable expression of FPR2 in WT lung tissue and confirmed the absence of FPR2 in all six of the previously mentioned organs (Figure 1F).

The FPR2$^{-/-}$ mice showed amplified, age-related body weight (Figure 1G). Therefore, obesogenic aging was validated using quantitative magnetic resonance imaging, which determined body composition such as lean mass, fat mass, and water content (Figure 1H—J). Both WT and FPR2$^{-/-}$ male mice showed a 30% increase in lean mass from 2 to 7 months (Figure 1H). At 2 months, there was no significant difference in the overall fat mass between FPR2$^{-/-}$ and WT mice; however, at 7 months, FPR2$^{-/-}$ mice had a 92% increase in the fat mass in comparison with respective age-matched WT mice (Figure 1I). There was no difference in water content between the two groups (Figure 1J). To determine the cause of obesity in FPR2$^{-/-}$ mice, indirect calorimetry was performed at 4 months. The weight gain of FPR2$^{-/-}$ mice correlated with a 24% ($p < 0.05$) increase in food intake compared with WT mice, suggesting that in FPR2$^{-/-}$ mice, obesity could be associated with hyperphagia (Figure 1K). FPR2 is a primary resolution sensor for the safe clearance of inflammation, and its deletion induced sex-specific age-related obesity and increased mortality, so we determined the role of FPR2 in the life span, cardiorenal syndrome in aging, and after cardiac injury using FPR2$^{-/-}$ male mice.

Sex-specific life span analyses showed that FPR2$^{-/-}$ male mice died within 10 months, while FPR2$^{-/-}$ female mice seemed to be more resistant to obesity and displayed only 10% mortality within the same time frame (Supplementary Figure 3). Survival analyses show that the median life span of FPR2$^{-/-}$ mice male was 6.2 months. Similarly, the maximal life span was significantly lower (~60%, 7.46 months) compared with control mice, which are considered to live until 24—36 months (Supplemental Table 2). FPR2$^{-/-}$ male mice developed obesity with shortened survival when compared with their FPR2$^{-/-}$ female counterparts; therefore, further experiments were performed using only male mice. Our results suggest that FPR2 expression is activated in the human ischemic myocardium and that the lack of FPR2 shortens the life span in male mice with the development of age-related obesity.

3.2. Absence of FPR2 impaired myocardium strain and promoted obesity-induced diastolic dysfunction

Because the FPR2 deletion in mice increased fat mass accumulation from an early age (Figure 1I), we measured age-associated cardiac function to gain insight into whether obesity superimposed on aging affected cardiac function. Echocardiography measurement of WT and

FPR2$^{-/-}$ mice at 2 and 7 months using B-mode speckle tracking, longitudinal three-dimensional (3D) strain, and synchronicity revealed dynamic changes in the LV with increased end-diastolic volume (91 $\pm$ 8 μL and end-systolic volume (43 $\pm$ 5 μL) in FPR2$^{-/-}$ mice at 7 months compared with age-matched WT controls (end-diastolic volume: 63 $\pm$ 6 μL; end-systolic volume: 28 $\pm$ 5 μL; Supplemental Tables 3A–B). Both 2- and 7-month-old FPR2$^{-/-}$ mice LV images of the B-mode long axis showed shortened green vectors and decreased in myocardial strain, indicative of LV dysfunction (Figure 2A; LV arrested in mid-systole). Heart dyssynchrony began at 2 months in the mid-anterior and apex (yellow and magenta line) in FPR2$^{-/-}$ mice and was further amplified at 7 months of age. In addition, cardiac dysfunction in 7-month-old FPR2$^{-/-}$ mice increased with progressive dyssynchrony in the anterior base (dark blue), mid-anterior (yellow), and posterior base (green) compared with age-matched WT controls. The presented results show that FPR2 deletion advanced LV dysfunction with marked impairment in myocardium strain and synchronicity as well as signs of LV age-related structural pathology (Supplementary Figure 2B). We further investigated whether the development of age-related cardiomyopathy of obesity advanced to heart diastolic and strain dysfunction since the systolic functional marker ejection fraction (EF%) showed limited changes in FPR2$^{-/-}$ mice compared with WT mice (Figure 2B).

Global longitudinal strain (GLS) is considered the standard measurement in HF patients [23]. In FPR2$^{-/-}$ mice, the GLS was increased by 3% at 2 months and 12% at 7 months compared with WT controls, which remained relatively unchanged from 2 to 7 months (Figure 2C). As shown in 3D strain images, the GLS of FPR2$^{-/-}$ mice shifted toward the positive (red), suggestive of systolic dysfunction, compared with the age-matched WT controls (Figure 2A,C). To assess diastolic function, mitral inflow Doppler velocity ratios (E/A, E′/A') in FPR2$^{-/-}$ and WT mice were determined using tissue Doppler echocardiography. Doppler data suggested a limited decrease of E/A but significant decrease of E′/A' ratios in FPR2$^{-/-}$ mice at 7 months compared with age-matched WT controls (Figure 2D–E). Doppler mode images of FPR2$^{-/-}$ mice exhibited an irregular diastolic septal annular wall motion, indicative of diastolic dysfunction at both 2 and 7 months compared with age-matched WT controls (Figure 2F). Thus, lack of FPR2 impaired myocardium strain and showed signs of cardiomyopathy in obesity with advanced diastolic dysfunction when obesity was superimposed on aging.

3.3. FPR2 deletion leads to obesity-induced cardiac aging with the implication of the integrin signaling pathway

Since FPR2 dysfunction drives obesogenic aging and diastolic dysfunction, we assessed whether obesity and aging affected the extracellular matrix (ECM) scaffold. ECM is an important determinant of the structural integrity of the myocardium and actively participates in force transmission across the LV wall. We quantified a panel of 84 ECM remodeling and adhesion genes in the LV of 7-month-old FPR2$^{-/-}$ mice and age-matched WT controls (Supplementary Figure 4). Of the total 84 genes, 45 were modulated in FPR2$^{-/-}$ 7-month-old mice compared with WT mice (Figure 3A). The 23 genes were upregulated while 15 genes were downregulated in FPR2$^{-/-}$ aging LV compared with the age-matched WT mice. Particularly, *integrin-α L* (itgal, 6.22-fold, $p < 0.01$) and matrix metallopeptidase (MMP) mRNA expression were increased in aging FPR2$^{-/-}$ mice compared with WT mice, whereas endogenous MMP inhibitors such as *Timp1* and disintegrins,

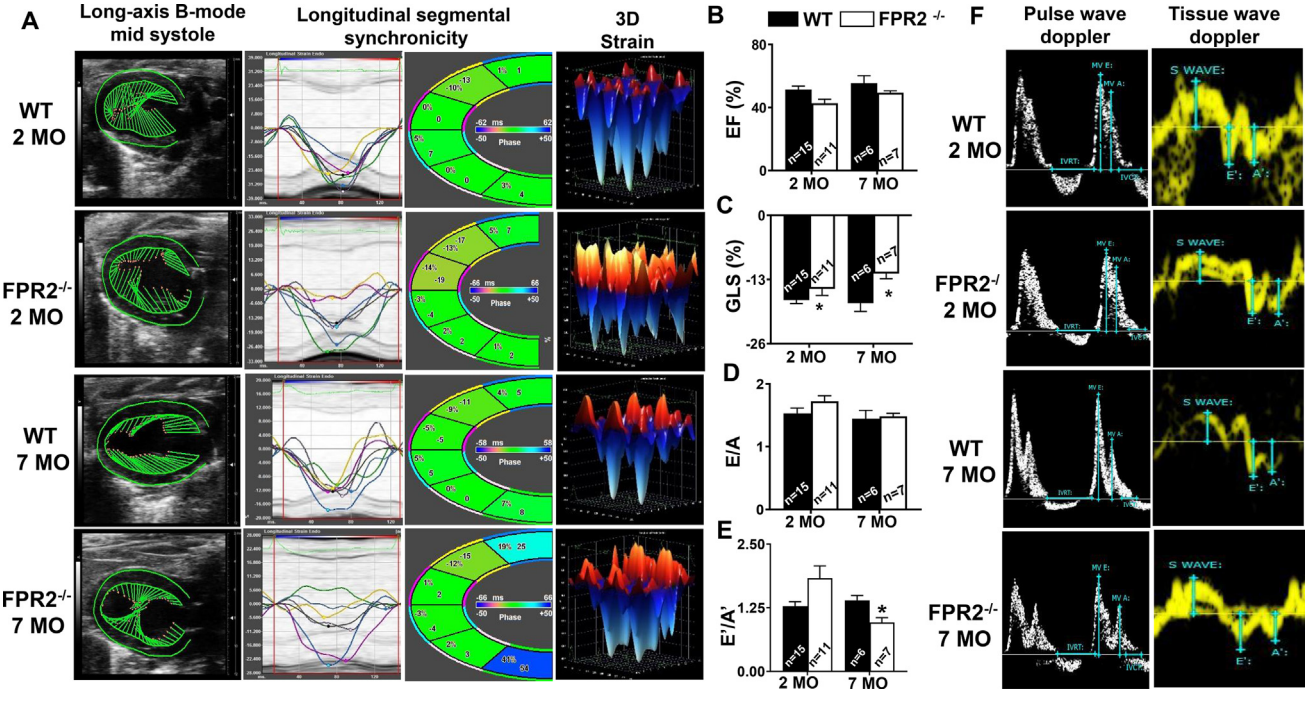

Figure 2: Deficiency of FPR2 impaired global myocardial strain and advanced age-related obesity-induced cardiac dysfunction measured using high-resolution echocardiography. (A) Echocardiographic speckle tracking–based LV systolic function analysis showing the change in the LV size, shape, and function in WT and FPR2$^{-/-}$ mice compared with the age-matched control group at 2 and 7 months of age (left to right panel: long axis B-mode, longitudinal segmental synchronicity, and 3D longitudinal strain). Bar graph representing **(B)** ejection fraction (EF%), **(C)** global longitudinal strain (GLS%), **and (D, E)** mitral inflow Doppler velocities ratios (E/A, E′/A'). **(F)** Representative images of pulse wave Doppler images (white) and tissue wave Doppler images (yellow) from WT and FPR2$^{-/-}$ mice at 2 and 7 months of age. Data are means $\pm$ SEM (n = 6–15 mice/group). *$p < 0.05$ vs respective control group.

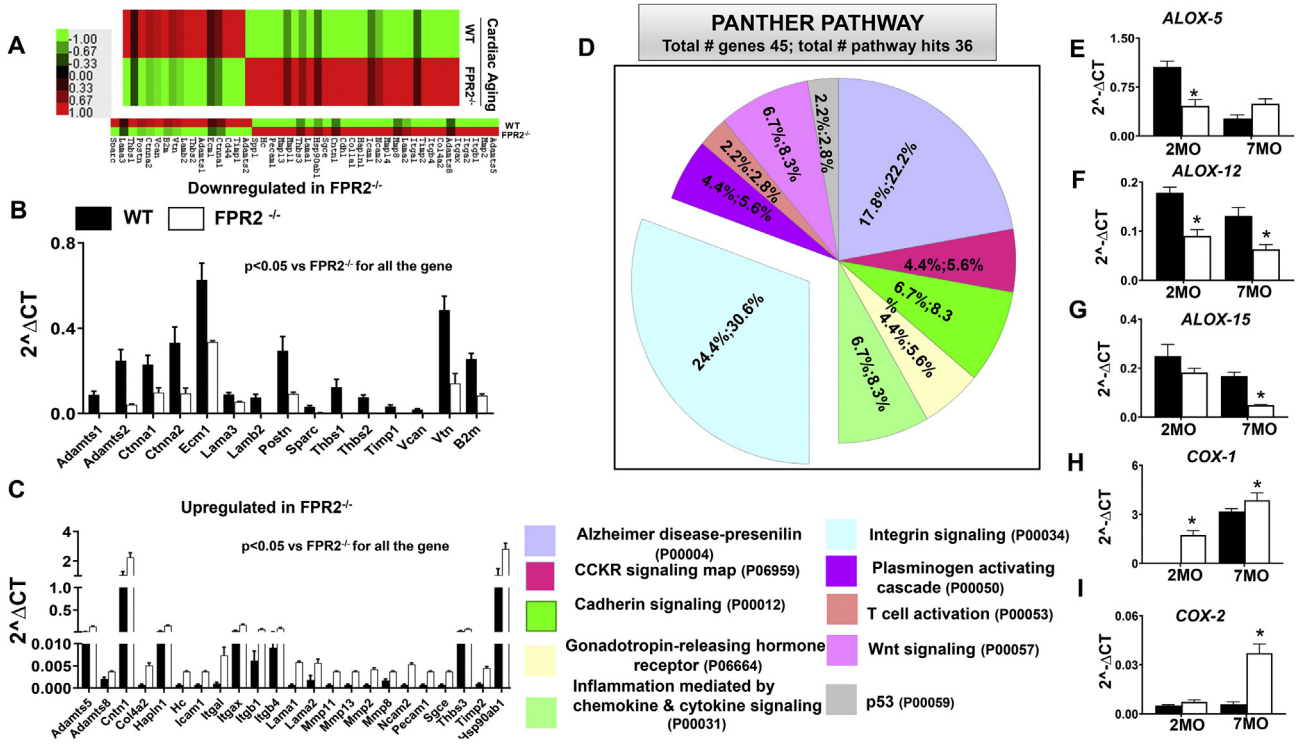

Figure 3: Deletion of FPR2 in mice advances cardiac aging with disruption in the integrin signaling pathway. (**A**) Heat map representing changes in the extracellular matrix (ECM) gene expression profile in WT and FPR2$^{-/-}$ mice at 7 months of age. Color-coded bar graph representing the change in expression from green (−1 lowest decrease) to red (+1 highest increase). Bar graph representing significantly **(B)** downregulated and **(C)** upregulated ECM genes in FPR2$^{-/-}$ mice compared with WT at 7 months of age. **(D)** Functional classification of genes using panther pathway analysis showing FPR2 deletion affected the integrin signaling pathway. **(E, F, G)** Decreased mRNA expression of immune-responsive *LOXs* (*ALOX-5*, *ALOX-12*, *ALOX-15*) in the LV of FPR2$^{-/-}$ mice at 2 and 7 months of age compared with WT. **(H, I)** Increased mRNA expression of *COX-1* and *COX-2* in the LV of FPR2$^{-/-}$ mice at 2 and 7 months of age as compared with WT. n = 5 mice per group; *$p < 0.05$ vs corresponding age-matched controls.

such as *Adamts1* and *Adamts2*, were decreased (Figure 3B,C). The Panther pathway analysis demonstrated that 7 different signaling pathways were highly affected in FPR2$^{-/-}$ aging mice compared with age-matched WT controls. The pie chart distribution showed that a significant number of genes were in favor of the integrin signaling pathway and were disrupted by FPR2 deletion (Figure 3D).

To examine whether obesity with aging drives cardiac inflammation in FPR2$^{-/-}$ mice, the expression of COXs (*COX-1, -2*) and arachidonate lipoxygenases (LOXs: *ALOX-5, -12, -15*) was quantified in the LV at 2 and 7 months in FPR2$^{-/-}$ and WT mice. In concordance with inflamed LV ECM data, we found that deletion of FPR2 dysregulated immune-responsive LOX and COX enzymes. FPR2 deletion decreased the levels of LOXs at 2 months. We noted significant decreases in the levels of *ALOX-12* (−0.5 fold) and *ALOX-15* (−0.3 fold; Figure 3E—G). Of note, FPR2 deletion overamplified LV proinflammatory COXs, with a 1.21-fold and 5.5-fold increase in *COX-1* and *COX-2* compared with age-matched WT controls at 7 months (Figure 3H—I). Together, these results indicate that obese aging drives cardiac inflammation with marked activation of immune-responsive COXs, deactivation of LOXs, and dysregulation of ECM signaling, which leads to low-grade chronic inflammation in FPR2$^{-/-}$ mice.

3.4. FPR2 deletion advanced age-related renal inflammation and fibrosis

Deletion of FPR2 induced obesity and impaired cardiac strain and advanced diastolic dysfunction with signs of advanced cardiac aging. We further evaluated whether FPR2 deletion leads to cardiorenal inflammation in aging mice. We evaluated the markers of inflammation in the LV of 2-month-old and 7-month-old FPR2$^{-/-}$ and WT age-matched control mice. mRNA expression of proinflammatory markers *CCL-2* (30-fold; Figure 4A), *IL-1β* (1.26-fold; Figure 4B), and *TNF-α* (0.51-fold; Figure 4C) were significantly upregulated at 7 months in the LV of FPR2$^{-/-}$ mice compared with the WT mice, showing signs of cardiac inflammation. These data led us to examine whether FPR2 deletion induced age-related renal inflammation. The kidneys of FPR2$^{-/-}$ mice revealed progressive inflammation compared with WT mice, which was confirmed by periodic acid—Schiff staining (Figure 4D), nephrin staining (Supplementary Figure 5D), and plasma creatinine, a kidney injury biomarker (Figure 4E). The kidney injury markers, such as NGAL, were increased at an early age in FPR2 mice, which is suggestive of inflamed kidneys. In correlation with these results, at 7 months, FPR2$^{-/-}$ mice upregulated the mRNA expression of *NGAL* (10-fold; Figure 4F), *KIM-1*, and *IL-1β* (1.2- and 8-fold, respectively; Supplementary Figure 5E—F) compared with WT mice. Furthermore, aging FPR2$^{-/-}$ mice showed an increase in fibrosis in the cortex compared with WT mice (Figure 4G—H). We assessed the kidney structural markers by immunofluorescence using WGA, vimentin, and NGAL (Figure 4I—K). The results were indicative of elevated chronic kidney injury. FPR2 deletion increased *CCL2* (7.3-fold; Figure 4L) *IL-1β* (2-fold; Figure 4M), and *TNF-α* (1.2-fold; Figure 4N) expression in the kidney at 7 months of age, indicating obesity-mediated renal syndrome in FPR2$^{-/-}$ aging mice. We further assessed whether FPR2 deletion contributes to nonresolving renal inflammation in cardiac injury. The upregulation of a kidney-specific

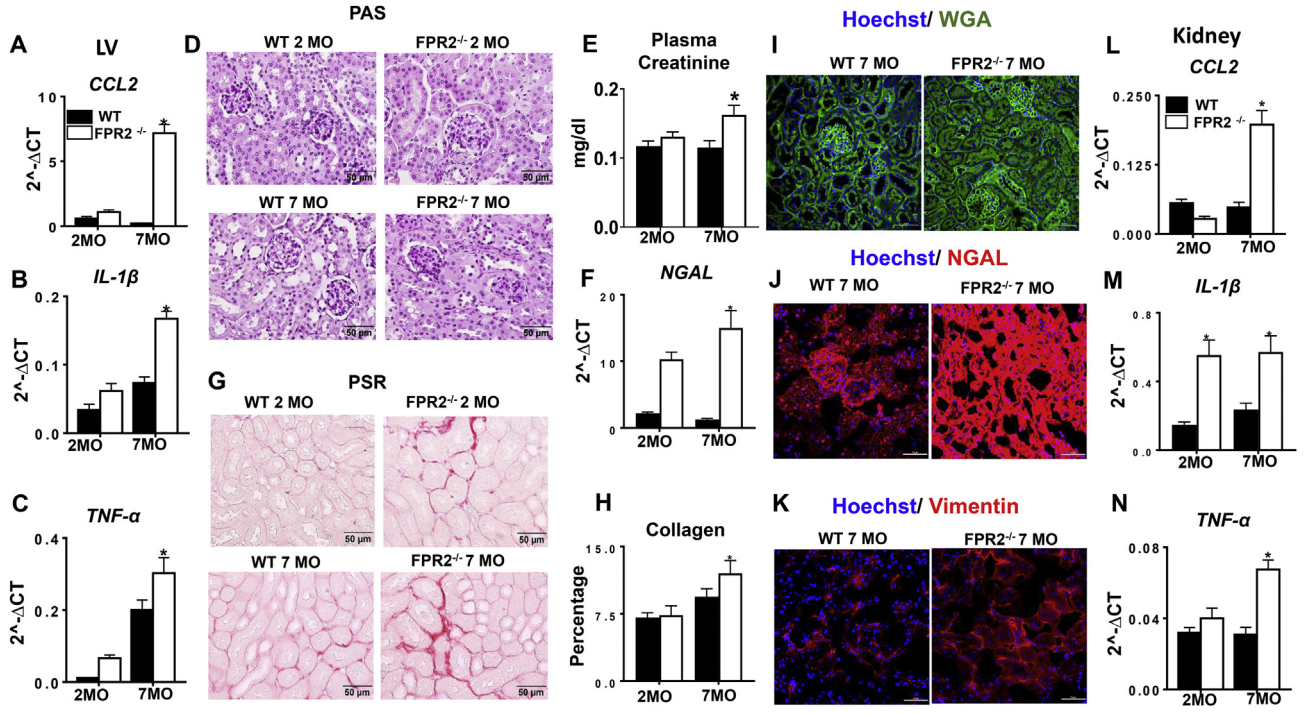

Figure 4: FPR2 deletion developed age-related cardiorenal syndrome with signs of unresolved and chronic inflammation. **(A, B, C)** mRNA expression profiling of proinflammatory cytokines (*Ccl2*, *IL1-β*, and *TNF-α*) in the LV of FPR2$^{-/-}$ and WT mice. **(D)** Periodic acid—Schiff (PAS) staining showing structural changes in the kidney at 7 months of age in WT and FPR2$^{-/-}$ mice (magnification = 40×; scale = 50 μm). **(E)** Increased plasma creatinine levels in FPR2$^{-/-}$ mice compared with WT at 7 months of age. **(F)** Kidney mRNA expression of injury marker NGAL in WT and FPR2$^{-/-}$ mice at 2 and 7 months of age. **(G)** Picrosirius red (PSR)—stained kidney showing fibrotic remodeling and collagen deposition in FPR2$^{-/-}$ mice at 2 and 7 months compared with age-matched WT controls (magnification = 40×; scale = 50 μm). **(H)** High collagen content in the cortex area of the kidney in FPR2$^{-/-}$ mice compared with WT mice at 2 and 7 months of age. **(I, J, K)** Immunofluorescence images presenting altered kidney structure stained using WGA (green), increased NGAL (red), and vimentin (red) staining in FPR2$^{-/-}$ mice compared with WT controls at 7 months of age. Nuclei are stained blue with Hoechst (magnification = 40×; scale = 50 μm). **(L, M, N)** mRNA expression of proinflammatory genes (*Ccl2*, *IL1-β*, and *TNF-α*) in the kidney of FPR2$^{-/-}$ and WT mice at 2 and 7 months of age. *$p < 0.05$ vs WT. Values are means ± SEM; n = 5—9 mice/group.

injury marker, NGAL protein expression in FPR2$^{-/-}$ mice confirmed renal inflammation at day 1 and 5 after MI (Supplementary Figure 5A). Our results demonstrated that FPR2 dysfunction induced an integrative and systemic inflammatory and fibrotic response in obesogenic aging.

3.5. Deletion of FPR2 deactivated LOXs and overactivated COXs with lowered SPMs in the infarcted LV after MI

FPR2 deletion amplified inflammation with aging as indicated by an increase in COXs and proinflammatory cytokines in the LV without any injury. Therefore, we aimed to determine the mechanism of FPR2-mediated defective cardiac healing after MI. After ischemic injury, splenic leukocytes mobilize to the infarcted myocardium to biosynthesize SPMs and facilitate clearance of deceased myocytes [24]. The SPM metabolome was determined in infarcted LV after MI using mass spectrometry. After MI, successful infarction of the LV was confirmed using echocardiography. Both FPR2$^{-/-}$ and WT mice showed an EF <20%, indicative of acute decompensated HF post-MI. The LV posterior wall thinning was confirmed using histology (Supplementary Figure 6A—B; Supplemental Table 3A). The overall percentage of SPMs was lower (30%) in the FPR2$^{-/-}$ mice compared with the WT mice, which had 70% of SPMs in the total distribution (Figure 5A). Detailed analysis of arachidonic acid (AA), docosahexaenoic acid (DHA), and eicosapentaenoic acid (EPA) revealed lower levels of fatty acids along with their respective metabolites (Figure 5B, Supplementary Figure 7A—C). The DHA metabolome displayed a significant decrease in resolvins, specifically RvD1, RvD4, MaR2, and AA-derived LXA_4 in the infarcted LV of FPR2$^{-/-}$ mice compared with WT mice (Figure 5C—I, Supplemental Table 4). The mRNA levels of SPMs biosynthesizing LOXs enzymes *ALOX15* and *ALOX5* were decreased in the infarcted LV compared with WT, which is consistent with the downregulation of SPMs (Figure 5J—K). COX-mediated prostaglandins and thromboxane were significantly lower in FPR2$^{-/-}$ infarcted LV; however, the mRNA levels of both COXs (*COX-1* and *COX-2*) were higher in the infarcted LV of FPR2$^{-/-}$ compared with WT mice, suggesting failed initiation of the inflammatory-resolving response after cardiac injury (Figure 5L—M).

3.6. Dysfunction of FPR2 lowered SPMs with impaired splenocardiac deactivation

Splenic monocyte-derived macrophages are a major contributor in the biosynthesis of SPMs following cardiac injury [25]. Asplenic patients show increased MI events and mortality from ischemic heart disease [26]; therefore, we quantitated leukocytes from the post-MI spleen and LV to determine macrophage-neutrophil populations and diversity. We quantitated the SPM resolution metabolome in spleen before MI. Similar to infarcted LV, results of the SPM metabolome analyses in the spleen revealed lower SPMs in FPR2$^{-/-}$ (38%) compared with WT, which displayed 62% of SPMs in total distribution pre-MI (Figure 6A). We delineated the detailed analysis of essential fatty acids (AA, DHA, and EPA) and quantified their mediators to define the cardiometabolic defects (Figure 6B). There was no change in DHA levels, but AA and EPA levels were lower in the FPR2$^{-/-}$ spleen compared with the WT

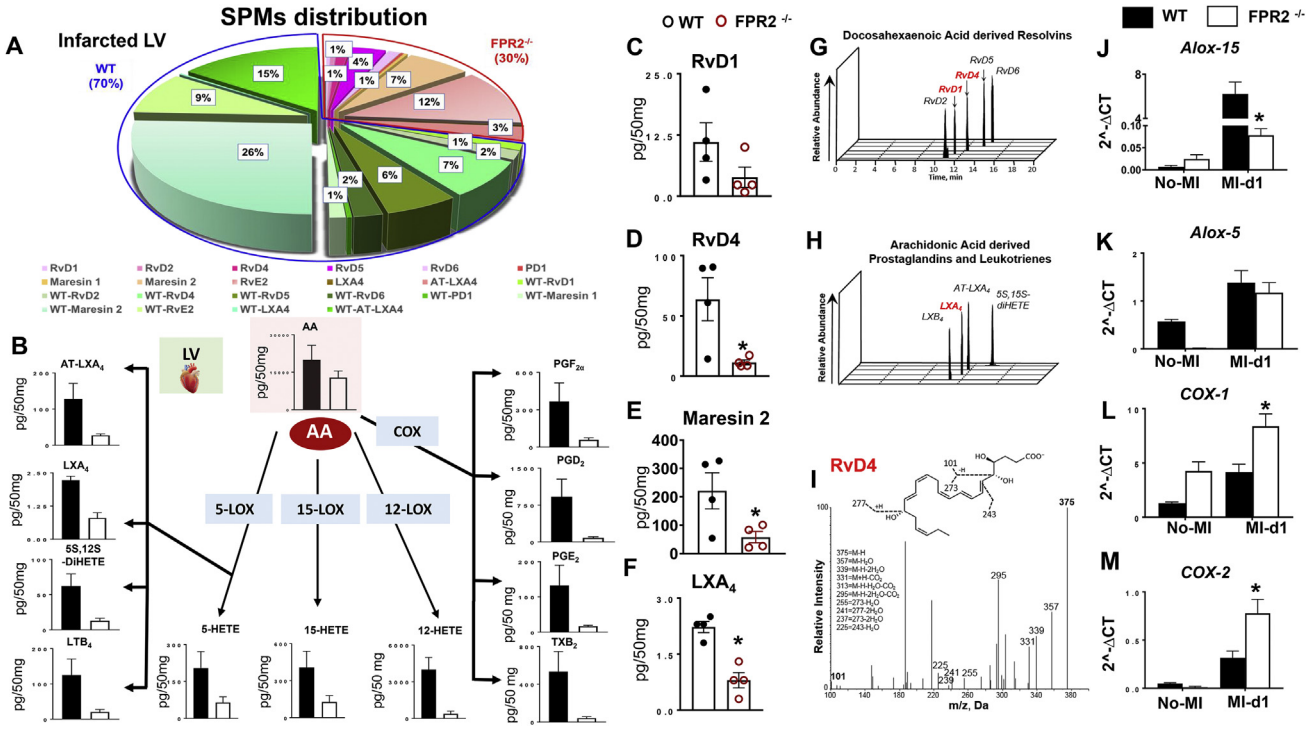

Figure 5: Dysfunction of FPR2 impaired SPM biosynthesis with dysregulation of LOXs and overactivation of COXs in the infarcted LV post-MI. (**A**) Pie chart representing the distribution of SPMs in WT and FPR2$^{-/-}$ mice at post-MI d1 in the infarcted LV. Percentage of mean values for each SPM moiety identified is presented in the pie chart. **(B)** Arachidonic acid (AA)—derived metabolome in the infarcted LV of WT and FPR2$^{-/-}$ mice post-MI at d1. **(C, D, E, F)** Decreased levels of SPMs (RvD1, RvD4, MaR2, and LXA$_4$) in the infarcted LV of FPR2$^{-/-}$ mice compared with WT at post-MI d1. **(G, H, I)** Representative multiple reaction monitoring chromatographs of DHA-derived resolvins, AA-derived prostaglandins, and leukotrienes and RvD4. Bar graphs representing LV mRNA expression of **(J, K)** *LOXs* and **(L, M)** *COXs* (*COX-1* and *COX-2*) at d1 post-MI. Values are means ± SEM; n = 4 mice per group in MI and no-MI controls. Quantification and values are pg/50 mg of LV tissue from apex to base. The detection limit was ∼1 pg.

mice (Supplementary Figure 8A—C). FPR2$^{-/-}$ mice showed lower splenic mRNA expression of LOXs (−5, −12, −15) and amplified COXs (−1 and −2) (Figure 6C—D). The detailed quantitation of the spleen AA metabolome showed AA-derived LOXs-directed bioactive mediators (AT-LXA$_4$, LXA$_4$, 5S,12S-diHETE, LTB$_4$, 5-HETE, 15-HETE, and 12-HETE) were relatively lower in FPR2$^{-/-}$ mice compared with WT. In contrast, despite higher COX expression, no change was observed in COX-derived mediators (PGF$_{2\alpha}$, PGD$_2$, and PGE$_2$, TXB$_2$) in FPR2$^{-/-}$ mice compared with WT (Figure 6B, Supplemental Table 4). Although DHA levels remained unchanged in the FPR2$^{-/-}$ spleen compared with WT, the DHA-derived bioactive mediators 4-, 7-, 14-, and 17-HDHA (hydroxydocosahexaenoic acid) were lower in the FPR2$^{-/-}$ spleen compared with the WT spleen (Supplementary Figure 8A—B). The overall EPA levels were decreased in the FPR2$^{-/-}$ spleen compared with the WT spleen (Supplementary Figure 8A—C). Together, quantitative analyses of resolution metabolome pre-MI suggested lower SPMs in FPR2$^{-/-}$ mice spleens compared with WT spleens with minimal influence on SPM precursor fatty acids.

3.7. FPR2 agonist resolvin D1 failed to activate macrophages, indicating nonresolving inflammation in resolution sensor—deficient mice

Since FPR2$^{-/-}$ mice showed lower SPMs in spleen before MI and in the infarcted LV after MI, we investigated the functional capacity of macrophages to determine the mechanism of nonresolving inflammation. As proresolving lipid agonists, resolvins are ligands that allow FPR2 to initiate the resolving response. To validate whether resolvin D1 (RvD1) operates in the absence of FPR2, we isolated peritoneal macrophages from WT and FPR2$^{-/-}$ mice and then sensitized macrophages with RvD1 treatment. RvD1 activated FPR2 in WT macrophages, suggestive of agonist action. This was demonstrated by an increase in FPR2 expression and translocation to the cytoplasm (purple), which is essential for pharmacological activity (Figure 6E). The nonactivation of the resolution sensor in FPR2$^{-/-}$ macrophages further confirmed FPR2 deletion (Figure 6E). The macrophage phenotype was confirmed using an F4/80 marker (green). We further stimulated WT and FPR2$^{-/-}$ peritoneal macrophages with lipopolysaccharide (LPS) and RvD1 to study proinflammatory and proresolving responses. Either proinflammatory (LPS)— or proresolving (RvD1)—treated macrophages from FPR2$^{-/-}$ mice failed to activate *TNF-α* and *IL-1β* cytokines compared with both unstimulated FPR2$^{-/-}$ and WT macrophages (Figure 6F). Macrophages isolated from FPR2$^{-/-}$ mice showed lower mRNA expression of proresolving genes *MRC-1* and *ARG-1* when compared with WT control (Figure 6F). Macrophage function was assessed by evaluating their ability to phagocytose *Escherichia coli* (red) ex vivo. The isolated peritoneal macrophages from FPR2$^{-/-}$ mice delayed the beginning of the phagocytic response when compared with WT macrophages. The WT macrophage phagocytosis started at the 15-minute time point, whereas the FPR2$^{-/-}$ macrophage activity began at the 30-minute time point, indicative of a deferred activation of the phagocytic process (Supplementary Figure 9A—B). FPR2$^{-/-}$ macrophages failed to activate the initial cytokine response in the presence of the proinflammatory/proresolving stimulus, thereby delaying the response to pyrogenic inflammation and further showing the defective phagocytosis process of *E. coli*.

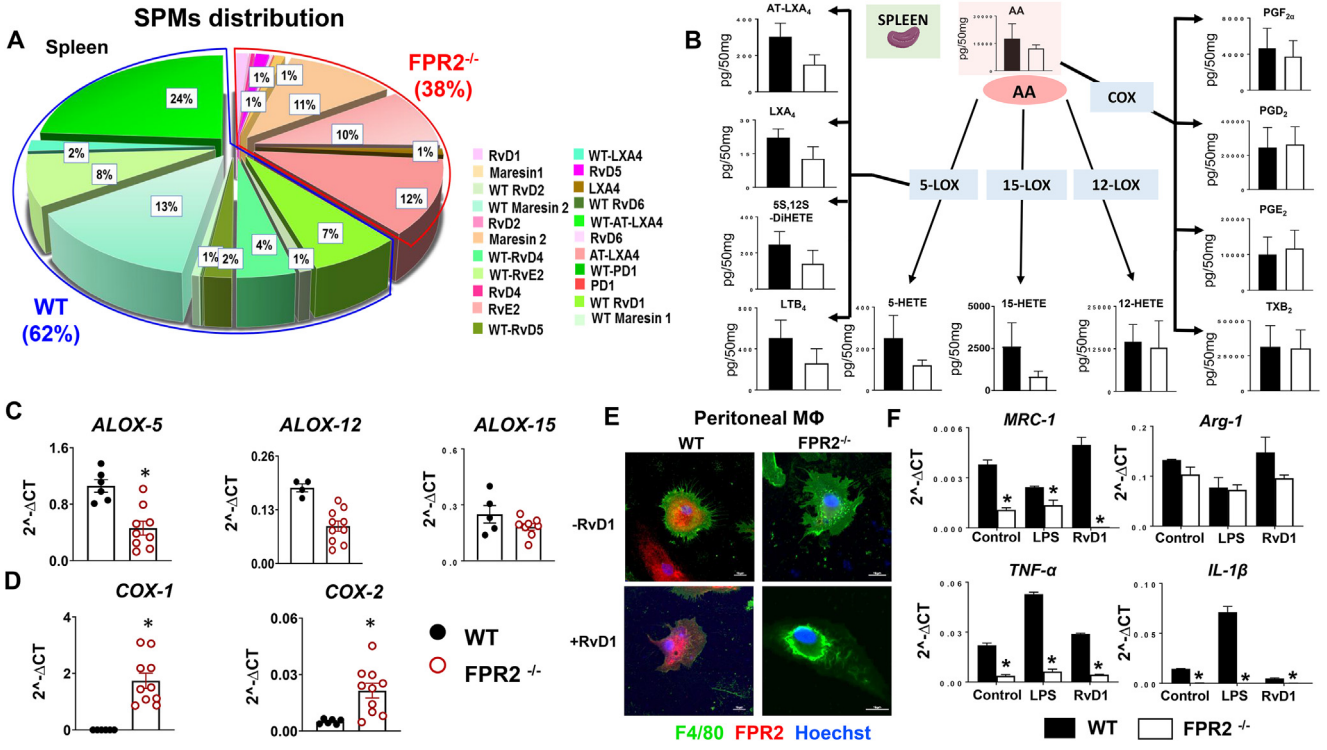

Figure 6: Lack of FPR2 dysregulated macrophages to initiate cytokine response *in vitro* with lower SPMs in the spleen in vivo. **(A)** Pie chart representing SPM distribution in WT and FPR2$^{-/-}$ mice in the spleen at d0. The percentage is the averaged mean for each SPM in the pie chart; n = 4 mice/group. Quantification and values are pg/50 mg of spleen tissue. The detection limit was ~1 pg. **(B)** Arachidonic acid (AA)—derived metabolome network in the spleen at d0. *n* = 4 mice/group. Splenic mRNA expression of immune-responsive **(C)** *LOXs* (*ALOX-5, ALOX-12, ALOX-15*) and **(D)** *COXs* (*COX-1, COX-2*) in WT and FPR2$^{-/-}$ mice at 2 months of age. Values are means ± SEM; n = 5–6 mice/group, *$p < 0.05$ vs WT. **(E)** Immunofluorescence images showing FPR2 expression (red) and translocation in response to RvD1 treatment in FPR2$^{-/-}$ mice compared with WT mice. Macrophage phenotype was confirmed using F4/80 (green). Nuclei are stained with Hoechst (blue). Images are representative of 3 experiments done in duplicate (magnification = 40×). **(F)** mRNA expression of proresolving (*MRC-1*, *ARG-1*) and proinflammatory (*TNF-α* and *IL-1β*) with or without LPS and RvD1 treatment in peritoneal macrophages isolated from FPR2$^{-/-}$ and WT mice. Values are means ± SEM; n = 6 mice; *$p < 0.05$ vs respective control.

3.8. Resolution sensor FPR2 deletion triggered splenocardiac nonresolving inflammation

Splenic leukocyte-directed SPMs biosynthesis is essential for cardiac healing, and FPR2$^{-/-}$ mice displayed lower levels of SPMs in the spleen prior to MI and in the infarcted LV post-MI. In humans, asplenic patients show amplified MI events and mortality from ischemic heart disease [26]. Therefore, we quantitated leukocytes from the spleen and LV post-MI in FPR2$^{-/-}$ mice to determine the macrophage-neutrophil population and their diversity [24]. A detailed flow cytometry gating strategy is provided in Supplementary Figure 10). After cardiac injury, splenic leukocyte activation is the first step for resolution of inflammation. Flow cytometry data showed that there was no difference in splenic and the LV percentage population of monocytes (CD45^{+}/CD11b^{+}) between WT and FPR2$^{-/-}$ mice after MI. Of note, FPR2$^{-/-}$ mice showed higher CD11b expression compared with WT in both spleen and LV post-MI (Figure 7A—D). The neutrophils are the first phagocytic responder in cardiac injury [5]. The splenic and LV neutrophil population (Ly6G^{+}) was significantly higher in FPR2$^{-/-}$ mice compared with WT post-MI. The splenic Ly6G^{+} cells showed 0.75 ± 0.3% in FPR2$^{-/-}$ mice compared with WT, which displayed 0.65 ± 0.03%. (Figure 7E). The infarcted LV Ly6G^{+} population was 10.02 ± 2.4% in FPR2$^{-/-}$ mice compared with 4.7 ± 0.3% in WT mice post-MI (Figure 7F). Of note, LV-Ly6G^{+} expression was lower in FPR2$^{-/-}$ mice compared with WT mice, indicating the presence of immature neutrophils (Figure 7H). Macrophages primarily biosynthesize SPMs in cardiac healing and facilitate clearance of inflammation. The macrophage cell population (CD45^{+}CD11b^{+} F4/80^{+}) and expression were similar in both the LV and spleen of WT and FPR2$^{-/-}$ mice post-MI (Figure 7I—L). Because the macrophage population was unaffected after MI, we further categorized them based on Ly6C^{low} and Ly6C^{high} expression. FPR2$^{-/-}$ mice had significantly decreased reparative Ly6C^{low} macrophages in both the spleen (1.33 ± 0.03%) and LV (5.53 ± 1.58%) compared with WT (spleen: 1.89 ± 0.16%; LV: 9.52 ± 1.07%; Figure 7M—P). Thus, deletion of FPR2 impaired timely activation of splenocardiac monocytes and macrophages, indicative of a dysregulated inflammation-resolution response in acute, decompensated HF post-MI.

4. DISCUSSION

The role of FPR2 in platelet biology and atherosclerosis has been reported previously [25,27]. The current study identified the integrative and interorgan link of FPR2 in obesogenic cardiac aging. This study also highlights that FPR2 dysfunction impaired SPM levels in the spleen pre-MI and lowered SPM levels in the infarcted LV post-MI. We used a series of novel and quantitative approaches that uncovered the following: (1) a lack of FPR2 led to age-associated cardiometabolic stress and diastolic dysfunction of the heart, (2) deletion of FPR2 magnified age-related inflammation and renal syndrome with modulation in the integrin signaling pathway, and (3) the absence of the resolution sensor FPR2 showed a splenocardiac resolution deficit in the infarcted myocardium in acute HF post-MI. Based on these

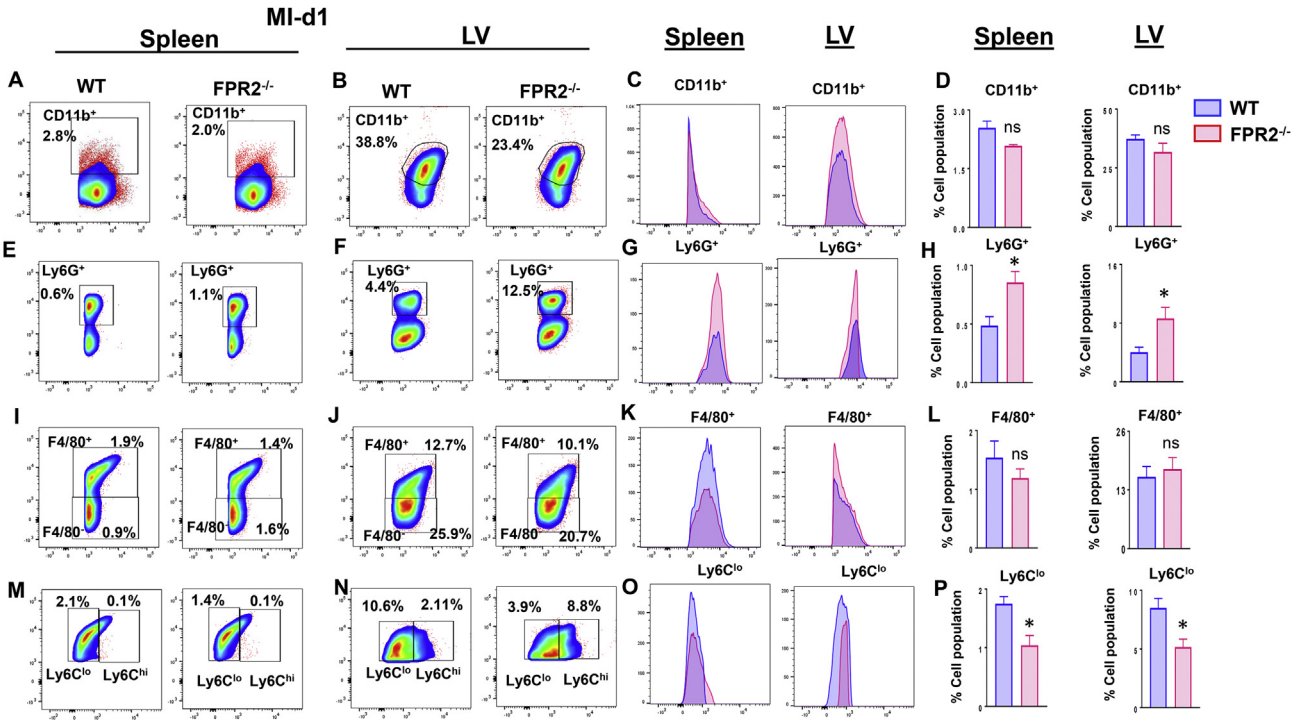

Figure 7: Deficiency of FPR2 impaired leukocyte phenotypes post-MI. Flow cytometry (FACs) pseudo plots representing monocyte populations ($CD45^+/CD11b^+$) in WT and $FPR2^{-/-}$ mice at post-MI d1: **(A)** spleen-$CD11b^+$, **(B)** LV-$CD11b^+$ population. **(C)** Histogram displaying $CD11b^+$ expression of spleen and LV. **(D)** Percentage of $CD11b^+$ population in spleen and LV. **(E)** Splenic neutrophils ($CD45^+/CD11b^+/F4/80^-/Ly6G^+$). **(F)** LV-$Ly6G^+$. **(G)** Histograms representing $Ly6G^+$ expression of spleen and LV. **(H)** Percentage of $Ly6G^+$ population in spleen and LV. Flow cytometry (FACs) pseudo plots representing macrophage populations ($CD45^+/CD11b^+/F4/80^+$) in WT and $FPR2^{-/-}$: **(I)** splenic macrophages ($F4/80^+$) and **(J)** LV macrophages ($F4/80^+$) post-MI. **(K)** Histograms representing $F4/80^+$ expression in WT and $FPR2^{-/-}$ spleen and LV. **(L)** Percentage of $Ly6G^+$ population in the spleen and LV. **(M)** Splenic macrophage subpopulations ($F4/80^+/Ly6C^{low/high}$). **(N)** LV macrophage subpopulations ($F4/80^+/Ly6C^{low/high}$). **(O)** Histograms displaying $Ly6C^{low/high}$ expression of the spleen and LV. **(P)** Percentage of $Ly6C^{low}$ population in the spleen and LV. $*p < 0.05$ vs WT. Values are means ± SEM; n = 4 mice/group.

observations, our study highlighted the critical role of the resolution sensor FPR2 in age-related cardiac dysfunction and the molecular mechanism of defective resolution in acute HF (Figure 8).

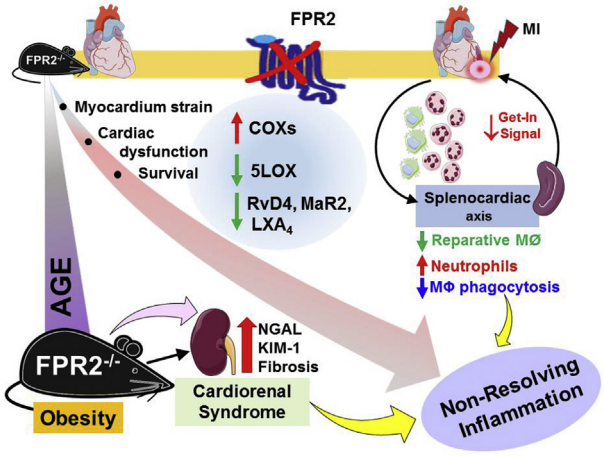

Figure 8: Summary sketch presenting splenocardiac resolution deficiency after cardiac injury and cardiorenal syndrome in FPR2-deficient obesity-prone mice. Male $FPR2^{-/-}$ mice developed age-associated obesity and reduced survival with signs of multiorgan nonresolving inflammation and cardiorenal syndrome during aging. After MI, splenocardiac resolution deficit was marked by the decrease in ALOX-5 expression and SPM reservoir in the infarcted LV with reduction of reparative macrophages and amplification of neutrophils.

4.1. FPR2 is essential for health and survival

In cardiovascular medicine discovery, survival is the hard endpoint that testifies to the therapy's value in humans. In the present report, obesity superimposed on aging advances to cardiometabolic syndrome with cardiac dysfunction of FPR2 mice, which is analogous to the main risk factor of obesogenic aging in humans. From an early age, the $FPR2^{-/-}$ mice began to accumulate fat mass with signs of obesity. With this obesity phenotype, the degree of the age-related metabolic disorder was confirmed using a life span assessment, which is relatively expensive and unfeasible in humans. The presented results indicate that the survival was sex specific, with significantly different survival rates observed in male and female $FPR2^{-/-}$ mice compared with age-matched WT male and female mice. Similar to diet-induced obesity in male C57BL/6J mice, $FPR2^{-/-}$ male mice are prone to obesity with impaired survival, which is suggestive of amplified multiorgan inflammation [28,29]. To our knowledge, this is the first comprehensive report that has determined the life span in $FPR2^{-/-}$ mice and reinforced obesity as one of the most common, noncommunicable diseases worldwide that affect cardiac function. The obesity-induced impairment of myocardium strain and diastolic dysfunction were readily apparent in both young and aging groups as compared with limited changes in systolic function. Obesity-induced cardiac dysfunction and signs of nonresolving inflammation in $FPR2^{-/-}$ mice qualify this as a "two-hit" model for the study of preserved ejection fraction or fractional shortening with an impaired diastolic function, which is common in age-related obese and/or diabetic mice and in the clinical setting [30,31].

4.2. Cardiac aging and cardiorenal syndrome

The amplified expression of inflammation mediating enzymes (COX-2 and COX-1) in the LV from an early age in the naïve state is another novel and unusual finding of this study. COXs not only generate prostaglandins but also aggravate inflammation, potentially dysregulating the ECM and inducing the installment of interstitial fibrosis [32]. In line with previous observations, FPR2 impairs integrin signaling along with the dysregulation of ECM [33–35]. In a model of sepsis, FPR2 dysfunctional mice intensified distant organ damage, particularly in acute kidney injuries [36]. Age-related findings support the indication that dysfunctional FPR2 triggers kidney pathology, which is confirmed histologically by increased collagenous fibrotic remodeling. As noted in the atherosclerotic study, FPR2 dysfunction favors vascular remodeling with the activation of MMP-13 and lowered TIMP1 collagen deposition in the murine smooth muscle cells of atherosclerotic lesions [37]. Kidney fibrotic remodeling was confirmed with a high plasma creatinine level and an increase in specific kidney injury markers, which are suggestive of sustained chronic inflammation related to a cardiorenal syndrome. As revealed in our previous study, obesity superimposed on aging desensitized FPR2, resulting in defective splenocardiac and cardiorenal network signaling pathways that promote nonresolving inflammation [22,34]. Thus, dysfunction of the FPR2 amplified the system-wide integrative cardiac pathology with intensified cardiorenal syndrome.

4.3. Splenocardiac resolution deficit and leukocyte phenotypes

Activated leukocyte expression of FPR2 serves as a resolution sensor for resolvins, lipoxins, and annexin A1. Recently, an additional role of FPR2 has been identified in the initiation of inflammation processes with the recruitment of chemotactic leukocytes ("get-in signal") and the regulation of the development of myeloid cells [16,38]. Here, we added three novel points: first, in FPR2-deficient mice, the sensitivity of macrophages to proinflammatory stimuli (LPS) and agonist (RvD1) is impaired with a lack of initiation of inflammation and failed activation of reparative markers. Second, after exposure to *E. coli*, FPR2$^{-/-}$ macrophages delayed the phagocytic response indicative of defective macrophage functions. Third, in line with the above Petri dish experiments, the FPR2$^{-/-}$ mice reduced the splenocardiac biosynthesis of SPMs in the infarcted heart, which could be due to the defective macrophage function in FPR2$^{-/-}$ mice [38]. Monocytes/macrophages are essential in early cardiac healing and repair when the balance between the splenic leukocyte release feedback and the feed-forward leukocyte-directed infarct clearance is maintained. After cardiac injury in FPR2$^{-/-}$ mice, leukocyte-enriched LOXs were reduced, decreasing SPM biosynthesis in the infarcted heart post-MI. In models of abdominal aortic aneurysm, FPR2$^{-/-}$ mice reduced ALOX-5, lowering the biosynthesis of SPMs in the infarcted heart [25]. Resolution sensor agonist RvD1 failed to activate macrophages, demonstrating impaired translocation in FPR2$^{-/-}$ macrophages [15]. Our previous report suggests that exogenous RvD1 treatment activates FPR2 at the splenic and infarcted sites with feed-forward biosynthesis of MaR1 and lipoxins post-MI to facilitate the resolution of inflammation [15]. Macrophage dysfunction and lower SPMs prior to MI in FPR2$^{-/-}$ mice could be a primary mechanism of splenocardiac resolution deficits after cardiac injury, because a clinical study demonstrated that spleen metabolic activity or splenectomy in humans defines the risk of future cardiovascular events and even mortality [26,39].

After ischemic injury, neutrophils offer the first line of defense to limit inflammation; however, in mice without FPR2, this leads to an expansion of premature neutrophils (Ly6G^{+}) in the spleen and LV, which is indicative of amplified collateral damage noticed in strokes, sepsis, and bacterial pneumonia [27,36,40]. In acute decompensated HF, splenic monocyte–derived macrophages direct SPM biosynthesis, but the lack of FPR2 impaired the biosynthesis of SPMs in the spleen pre-MI and at infarcted sites post-MI, reducing the reparative macrophages (Ly6C^{low}) in the infarcted heart [24]. Comprehensive analyses of macrophage subpopulations indicated high levels of proinflammatory macrophages (F4/80^{+}/Ly6C^{high}) in FPR2$^{-/-}$ mice with lower reparative Ly6C^{low} macrophages, which could be explained by the defective state of the splenic and peritoneal macrophages with impaired SPM biosynthesis. Dysfunction of FPR2 lowered LOXs and thereby the defective SPM biosynthesis that dysregulated the macrophage phenotype after cardiac injury, leading to a deficit in splenocardiac resolution in acute HF.

5. CONCLUSION

A lack of the resolution sensor FPR2 failed to initiate macrophage inflammatory and reparative responses in vitro and ex vivo. In vivo, FPR2 deletion induced cardiometabolic defects and cardiac dysfunction with reduced levels of SPMs in the infarcted heart and chronic inflammation in the cardiorenal network in aging. The dysregulation of LOXs and overactivation of COXs in the spleen and injured LV of FPR2$^{-/-}$ mice amplified the splenocardiac inflammation–resolution deficit with marked renal syndrome in aging. Thus, the presented results signify the integrative role of FPR2 as a primary target for managing cardiometabolic health, inflammation–resolution processes, and cardiorenal syndrome in aging.

AUTHOR CONTRIBUTIONS

G.V.H. conceived, designed, and executed the project. B.T., V.K., G.V.H., P.C.N., and A.B.P. conducted the experiments, contributed to the data analysis, and cowrote the paper with G.V.H., N.P., X.L., and C.N.S. All authors have critically revised the manuscript for intellectual content and approved its final version.

ACKNOWLEDGMENT

The authors acknowledge funding support from the National Institutes of Health (HL132989 and HL144788) to G.V.H. and the American Heart Association postdoctoral fellowship (POST31000008) to V.K. We acknowledge support from the UAB-UCSD O'Brien Core Center for Acute Kidney Injury Research (NIH GM095467), UAB Small Animal Phenotyping Core supported by the NIH Nutrition & Obesity Research Center (P30DK056336), and the Mouse Cardiovascular Core Vevo 3100 Mouse Ultrasound Facility for this project. C.N.S. and P.C.N. are supported by Program Project 5 P01 GM095467 from NIH/NIGMS. The authors acknowledge Actelion Pharmaceuticals Ltd (Switzerland) for providing the animals and Servier Medical Art gallery (creative common license), which was used to illustrate the study design and summary figures in the manuscript.

CONFLICT OF INTEREST

The authors declare no competing financial interests.

APPENDIX A. SUPPLEMENTARY DATA

Supplementary data to this article can be found online at https://doi.org/10.1016/j.molmet.2019.10.008.

REFERENCES

[1] Pai, J.K., Pischon, T., Ma, J., Manson, J.E., Hankinson, S.E., Joshipura, K., et al., 2004. Inflammatory markers and the risk of coronary heart disease in

men and women. New England Journal of Medicine 351:2599–2610. https://doi.org/10.1056/NEJMoa040967.

[2] Westman, P.C., Lipinski, M.J., Luger, D., Waksman, R., Bonow, R.O., Wu, E., et al., 2016. Inflammation as a driver of adverse left ventricular remodeling after acute myocardial infarction. Journal of the American College of Cardiology 67:2050–2060. https://doi.org/10.1016/j.jacc.2016.01.073.

[3] Pullen, A.B., Jadapalli, J.K., Rhourri-Frih, B., Halade, G.V., 2019. Re-evaluating the causes and consequences of non-resolving inflammation in chronic cardiovascular disease. Heart Failure Reviews. https://doi.org/10.1007/s10741-019-09817-x.

[4] Jessup, M., Brozena, S., 2003. Heart failure. New England Journal of Medicine 348:2007–2018. https://doi.org/10.1056/NEJMra021498.

[5] Kain, V., Prabhu, S.D., Halade, G.V., 2014. Inflammation revisited: inflammation versus resolution of inflammation following myocardial infarction. Basic Research in Cardiology 109:444. https://doi.org/10.1007/s00395-014-0444-7.

[6] Halade, G.V., Kain, V., Ingle, K.A., 2018. Heart functional and structural compendium of cardiosplenic and cardiorenal networks in acute and chronic heart failure pathology. American Journal of Physiology – Heart and Circulatory Physiology 314:H255–H267. https://doi.org/10.1152/ajpheart.00528.2017.

[7] Serhan, C.N., 2014. Pro-resolving lipid mediators are leads for resolution physiology. Nature 510:92–101. https://doi.org/10.1038/nature13479.

[8] Liu, M., Chen, K., Yoshimura, T., Liu, Y., Gong, W., Wang, A., et al., 2012. Formylpeptide receptors are critical for rapid neutrophil mobilization in host defense against Listeria monocytogenes. Scientific Reports 2:786. https://doi.org/10.1038/srep00786.

[9] Drechsler, M., de Jong, R., Rossaint, J., Viola, J.R., Leoni, G., Wang, J.M., et al., 2015. Annexin A1 counteracts chemokine-induced arterial myeloid cell recruitment. Circulation Research 116:827–835. https://doi.org/10.1161/circresaha.116.305825.

[10] Chiang, N., Serhan, C.N., Dahlen, S.E., Drazen, J.M., Hay, D.W., Rovati, G.E., et al., 2006. The lipoxin receptor ALX: potent ligand-specific and stereoselective actions in vivo. Pharmacological Reviews 58:463–487. https://doi.org/10.1124/pr.58.3.4.

[11] Brink, C., Dahlen, S.E., Drazen, J., Evans, J.F., Hay, D.W., Nicosia, S., et al., 2003. International Union of Pharmacology XXXVII. Nomenclature for leukotriene and lipoxin receptors. Pharmacological Reviews 55:195–227. https://doi.org/10.1124/pr.55.1.8.

[12] Back, M., Dahlen, S.E., Drazen, J.M., Evans, J.F., Serhan, C.N., Shimizu, T., et al., 2011. International Union of Basic and Clinical Pharmacology. LXXXIV: leukotriene receptor nomenclature, distribution, and pathophysiological functions. Pharmacological Reviews 63:539–584. https://doi.org/10.1124/pr.110.004184.

[13] Fiore, S., Maddox, J.F., Perez, H.D., Serhan, C.N., 1994. Identification of a human cDNA encoding a functional high affinity lipoxin A4 receptor. Journal of Experimental Medicine 180:253–260.

[14] Kain, V., Liu, F., Kozlovskaya, V., Ingle, K.A., Bolisetty, S., Agarwal, A., et al., 2017. Resolution agonist 15-epi-Lipoxin A4 programs early activation of resolving phase in post-myocardial infarction healing. Scientific Reports 7:9999. https://doi.org/10.1038/s41598-017-10441-8.

[15] Kain, V., Ingle, K.A., Colas, R.A., Dalli, J., Prabhu, S.D., Serhan, C.N., et al., 2015. Resolvin D1 activates the inflammation resolving response at splenic and ventricular site following myocardial infarction leading to improved ventricular function. Journal of Molecular and Cellular Cardiology 84:24–35. https://doi.org/10.1016/j.yjmcc.2015.04.003.

[16] Chen, K., Singh, V.K., Tang, P., Bao, Z., He, T., Xiang, Y., et al., 2018. Deficiency in Fpr2 results in reduced numbers of Lin(-)cKit(+)Sca1(+) myeloid progenitor cells. Journal of Biological Chemistry 293:13452–13463. https://doi.org/10.1074/jbc.RA118.002683.

[17] Ramon, S., Bancos, S., Serhan, C.N., Phipps, R.P., 2014. Lipoxin A(4) modulates adaptive immunity by decreasing memory B-cell responses via an ALX/FPR2-dependent mechanism. European Journal of Immunology 44:357–369. https://doi.org/10.1002/eji.201343316.

[18] Perretti, M., Chiang, N., La, M., Fierro, I.M., Marullo, S., Getting, S.J., et al., 2002. Endogenous lipid- and peptide-derived anti-inflammatory pathways generated with glucocorticoid and aspirin treatment activate the lipoxin A4 receptor. Nature Medicine 8:1296–1302. https://doi.org/10.1038/nm786.

[19] Perretti, M., D'Acquisto, F., 2009. Annexin A1 and glucocorticoids as effectors of the resolution of inflammation. Nature Reviews Immunology 9:62–70. https://doi.org/10.1038/nri2470.

[20] Corminboeuf, O., Leroy, X., 2015. FPR2/ALXR agonists and the resolution of inflammation. Journal of Medicinal Chemistry 58:537–559. https://doi.org/10.1021/jm501051x.

[21] Halade, G.V., Kain, V., Wright, G.M., Jadapalli, J.K., 2018. Subacute treatment of carprofen facilitate splenocardiac resolution deficit in cardiac injury. Journal of Leukocyte Biology 104:1173–1186. https://doi.org/10.1002/JLB.3A0618-223R.

[22] Halade, G.V., Kain, V., Black, L.M., Prabhu, S.D., Ingle, K.A., 2016. Aging dysregulates D- and E-series resolvins to modulate cardiosplenic and cardiorenal network following myocardial infarction. Aging (Albany NY) 8:2611–2634. https://doi.org/10.18632/aging.101077.

[23] Park, J.J., Park, J.B., Park, J.H., Cho, G.Y., 2018. Global longitudinal strain to predict mortality in patients with acute heart failure. Journal of the American College of Cardiology 71:1947–1957. https://doi.org/10.1016/j.jacc.2018.02.064.

[24] Halade, G.V., Norris, P.C., Kain, V., Serhan, C.N., Ingle, K.A., 2018. Splenic leukocytes define the resolution of inflammation in heart failure. Science Signaling 11. https://doi.org/10.1126/scisignal.aao1818.

[25] Petri, M.H., Thul, S., Andonova, T., Lindquist-Liljeqvist, M., Jin, H., Skenteris, N.-T., et al., 2018. Resolution of inflammation through the lipoxin and ALX/FPR2 receptor pathway protects against abdominal aortic aneurysms. JACC Basic to Translational Science. https://doi.org/10.1016/j.jacbts.2018.08.005.

[26] Robinette, C.D., Fraumeni Jr., J.F., 1977. Splenectomy and subsequent mortality in veterans of the 1939-45 war. Lancet 2:127–129.

[27] Vital, S.A., Becker, F., Holloway, P.M., Russell, J., Perretti, M., Granger, D.N., et al., 2016. Formyl-peptide receptor 2/3/lipoxin A4 receptor regulates neutrophil-platelet aggregation and attenuates cerebral inflammation: impact for therapy in cardiovascular disease. Circulation 133:2169–2179. https://doi.org/10.1161/circulationaha.115.020633.

[28] Xiang, Y., Yao, X., Chen, K., Wang, X., Zhou, J., Gong, W., et al., 2016. The G-protein coupled chemoattractant receptor FPR2 promotes malignant phenotype of human colon cancer cells. American Journal of Cancer Research 6:2599–2610.

[29] Surwit, R.S., Kuhn, C.M., Cochrane, C., McCubbin, J.A., Feinglos, M.N., 1988. Diet-induced type II diabetes in C57BL/6J mice. Diabetes 37:1163–1167.

[30] Valero-Munoz, M., Backman, W., Sam, F., 2017. Murine models of heart failure with preserved ejection fraction: a "fishing expedition. JACC Basic Translational Science 2:770–789. https://doi.org/10.1016/j.jacbts.2017.07.013.

[31] Schiattarella, G.G., Altamirano, F., Tong, D., French, K.M., Villalobos, E., Kim, S.Y., et al., 2019. Nitrosative stress drives heart failure with preserved ejection fraction. Nature 568:351–356. https://doi.org/10.1038/s41586-019-1100-z.

[32] Dearth, C.L., Slivka, P.F., Stewart, S.A., Keane, T.J., Tay, J.K., Londono, R., et al., 2016. Inhibition of COX1/2 alters the host response and reduces ECM scaffold mediated constructive tissue remodeling in a rodent model of skeletal muscle injury. Acta Biomaterialia 31:50–60. https://doi.org/10.1016/j.actbio.2015.11.043.

[33] Wantha, S., Alard, J.E., Megens, R.T., van der Does, A.M., Doring, Y., Drechsler, M., et al., 2013. Neutrophil-derived cathelicidin promotes adhesion

of classical monocytes. Circulation Research 112:792–801. https://doi.org/10.1161/circresaha.112.300666.

[34] Zannad, F., Rossignol, P., 2018. Cardiorenal syndrome revisited. Circulation 138:929–944. https://doi.org/10.1161/circulationaha.117.028814.

[35] Halade, G.V., Kain, V., Serhan, C.N., 2018. Immune responsive resolvin D1 programs myocardial infarction-induced cardiorenal syndrome in heart failure. The FASEB Journal 32:3717–3729. https://doi.org/10.1096/fj.201701173RR.

[36] Gobbetti, T., Coldewey, S.M., Chen, J., McArthur, S., le Faouder, P., Cenac, N., et al., 2014. Nonredundant protective properties of FPR2/ALX in polymicrobial murine sepsis. Proceedings of the National Academy of Sciences of the United States of America 111:18685–18690. https://doi.org/10.1073/pnas.1410938111.

[37] Petri, M.H., Laguna-Fernandez, A., Gonzalez-Diez, M., Paulsson-Berne, G., Hansson, G.K., Back, M., 2015. The role of the FPR2/ALX receptor in atherosclerosis development and plaque stability. Cardiovascular Research 105:65–74. https://doi.org/10.1093/cvr/cvu224.

[38] Maderna, P., Cottell, D.C., Toivonen, T., Dufton, N., Dalli, J., Perretti, M., et al., 2010. FPR2/ALX receptor expression and internalization are critical for lipoxin A4 and annexin-derived peptide-stimulated phagocytosis. The FASEB Journal 24:4240–4249. https://doi.org/10.1096/fj.10-159913.

[39] Emami, H., Singh, P., MacNabb, M., Vucic, E., Lavender, Z., Rudd, J.H., et al., 2015. Splenic metabolic activity predicts risk of future cardiovascular events: demonstration of a cardiosplenic axis in humans. JACC Cardiovascular Imaging 8:121–130. https://doi.org/10.1016/j.jcmg.2014.10.009.

[40] Sham, H.P., Walker, K.H., Abdulnour, R.E., Krishnamoorthy, N., Douda, D.N., Norris, P.C., et al., 2018. 15-epi-Lipoxin A4, resolvin D2, and resolvin D3 induce NF-kappaB regulators in bacterial pneumonia. The Journal of Immunology 200:2757–2766. https://doi.org/10.4049/jimmunol.1602090.

